J. Fluid Mech. (1975), *vol.* 68, *part* 3, *pp.* 503–512
Printed in Great Britain

The two-dimensional elliptical cap bubble

By J. H. HILLS

Department of Chemical Engineering, University of Cambridge†

(Received 16 May 1974)

A study of the closed wakes behind large gas bubbles rising between two parallel plates reveals that they are elliptical in shape, rather than circular. Fitting an arc of an ellipse, rather than a circle, to the curved upper surface of such a bubble eliminates a discrepancy between theory and experiment noted by Collins (1965*a*). Collins' analysis of the effect of finite channel width is extended to the elliptical case, and the stability of the closed wake is examined.

1. Introduction

Several experimental studies have been made of the rise of a large 'two-dimensional' bubble in liquid held between two flat plates (Collins 1965*a,b*; Grace & Harrison 1967; Crabtree & Bridgwater 1967).

The classic theory of Davies & Taylor (1950)may be applied to this situation. Liquid flow near the nose of the bubble is assumed to be given by potential flow over the forward part of a circular cylinder, for which the complex potential is

$$w = U(z+R^2/z), \tag{1}$$

where R is the radius of the cylinder and U the velocity of the distant flow relative to the cylinder. With the fluid velocity obtained from (1), Bernoulli's theorem with constant pressure on the dividing streamline gives

$$U = \tfrac{1}{2}(Rg)^{\frac{1}{2}}, \tag{2}$$

where R is the radius of the cylinder of which the bubble is a cap.

Collins (1965*a*) modified this approach to allow for the finite width of the bed. He replaced the second term on the right-hand side of (1), which represents the potential due to an unbounded doublet, with the potential due to a doublet lying between two planes at $z = \pm\tfrac{1}{2}iL$ (Lamb 1932, p. 71) to obtain

$$w = Uz + C\coth(\pi z/L), \tag{3}$$

where C is proportional to the strength of the doublet. Applying the analysis of Davies & Taylor to this case, he found

$$U = \left[\left(\tanh\frac{\pi a}{L}\right)\left(3-\tanh^2\frac{\pi a}{L}\right)\left(\frac{Lg}{12\pi}\right)\right]^{\frac{1}{2}}, \tag{4}$$

where a is the vertical half-diameter of the closed dividing streamline. Equation (4) reduces to (2) as $a/L \to 0$ (infinite bed). As $a/L \to \infty$ (narrow bed) the bubble

† Present address: Department of Chemical Engineering, University of Nottingham.

becomes a slug rising with a velocity determined entirely by the bed width. Equation (4) gives in this case

$$U = (Lg/6\pi)^{\frac{1}{2}}. \tag{5}$$

This result is in agreement with other theoretical values for slug velocity, apart from small differences in the numerical constant.

A comparison of experimental results with (4) showed that the former were some 9 % too high. Grace & Harrison (1967) found a similar discrepancy when they compared results in a wide bed with (2). Collins attributed the discrepancy to a residual three-dimensional effect.

In the course of a study of the motion of small bubbles swept round a large one (Hills 1971) we have re-examined the shape of a two-dimensional cap and its associated closed wake, and concluded that it is more nearly elliptical than circular. The experimental evidence is presented in § 2, while in § 3 we demonstrate that the use of potential flow round an elliptical cylinder to model the flow over the bubble cap removes the discrepancy noted above.

2. The nature of the wake

Davies & Taylor (1950) showed spark photographs of a spherical cap bubble in nitrobenzene which, owing to optical anisotropy of the liquid under shear, revealed a closed region of high shear immediately below the bubble, approximately completing the sphere. No other wake details were visible.

Maxworthy (1967) photographed two small spherical cap bubbles rising from coloured to clear water: the wake was turbulent for many diameters downstream and showed no evidence of a closed region.

Collins (1968) considered that Maxworthy's bubbles were too small to be true spherical caps, and presented a photograph of a larger bubble (40 ml) rising in water containing particles of soluble aspirin as tracers. A closed spherical region was again apparent. He also presented a photograph taken with the camera stationary to show the fluid streamlines, which were very similar to those due to an irrotational dipole, again suggesting steady flow over the region beyond a closed sphere. A narrow secondary wake was also visible, and the whole pattern was similar to flow round a sphere on which boundary-layer separation is delayed until the rear stagnation point or just before it.

Wegener & Parlange (1973) presented schlieren photographs of spherical caps rising in water which showed a turbulent region extending many bubble diameters downstream. Their bubbles were large enough to be true spherical caps and the apparent discrepancy with Collins' work is puzzling. It is possible that the fine detail of the schlieren technique obscures the broad flow patterns brought out by solid particles.

In two dimensions, Collins (1965*b*) reported a stable vortex pair behind a rising cylindrical cap, the closed figure being approximately circular in shape. However, Crabtree & Bridgwater (1967) found considerable wake shedding, with the formation of a vortex street. A closed wake was only observed in very viscous liquids, i.e. at small Reynolds numbers.

To attempt to clarify the situation, we have investigated the development of the wakes behind rising cylindrical cap bubbles of different sizes. The apparatus was formed from two plates of Perspex acrylic sheet 600 mm wide and 1200 mm high. The nominal separation of the plates was 9 mm, but in spite of being braced by steel bars, the Perspex bowed slightly and the actual bed thickness on the vertical centre-line varied from 9·5 mm at the top to 10·5 mm at the bottom. Bubbles of varying volume were injected by a cylindrical slide device, and the wake was made visible by adding dye to the water in the slide below the bubble. Details are given in Hills (1971). The rising bubble and wake were photographed with a ciné camera. In all cases, the bubble had a perfect closed wake during the initial stage of its rise (figure 1*a*, plate 1) but the wake was later shed in an irregular vortex street (figure 1*b*, plate 1.)

The smallest bubble used, of volume 5 ml, was not a perfect cylindrical cap (figure 1*b*). It rocked from side to side as it rose, and the wake shedding was associated with this rocking. For this bubble, the Reynolds number was $\simeq$ 8000 and the Weber number $\simeq$ 30 (based on the equivalent cylindrical diameter of the bubble). The Weber number for transition from an ellipsoidal to a spherical cap is given by Haberman & Morton (1953) as $Wb \simeq 20$, and by other workers as slightly higher, so there seems to be a close similarity between the two- and three-dimensional cases in this respect.

Larger bubbles did not rock; their wakes increased in size and became slightly more elongated as they rose. Eventually, portions of the coloured fluid at the edge of the wake appeared to 'roll off' towards the rear rather like a stocking being rolled off the leg. Here, they formed two long tails. The tails were normally of unequal length, and the longer one gradually curled up behind the remainder of the wake and was shed as the first vortex of the street. Determination of the precise onset of shedding is somewhat subjective, but figure 2 gives some indication of how this varies with bubble size. Collins' bubble had an equivalent diameter of about 40 mm, and according to figure 2 it should have become unstable at a height of about 400 mm. The fact that Collins noted no instability over the entire 900 mm of his bed height suggests that the thinner bed used in his work (6 mm) confers a greater stability on the wake.

Thus the closed wake seems to be a transient phenomenon in two-dimensional beds, occurring only during the initial part of the rise. However, even when wake shedding has started, the flow around the bubble cap and the upper part of the wake remains steady, and it is this flow which is considered in the remainder of the present paper.

When the closed wake exists, its shape is seen to be not perfectly circular, but elongated vertically. It is convenient to characterize this oval by means of the ratio of its vertical diameter $2a$ to its horizontal diameter $2b$. When wake shedding has started, the complete oval shape no longer exists, but the top half of the wake, including the bubble itself, still forms a semi-oval for which it is possible to estimate the semi-diameters a and b and calculate the axis ratio $\chi = a/b$. Figure 3 shows a graph of χ as a function of height for each of the five bubble sizes studied. We note that χ initially increases, but that the increase levels off when wake shedding starts. The results are very scattered, because of the difficulty in placing

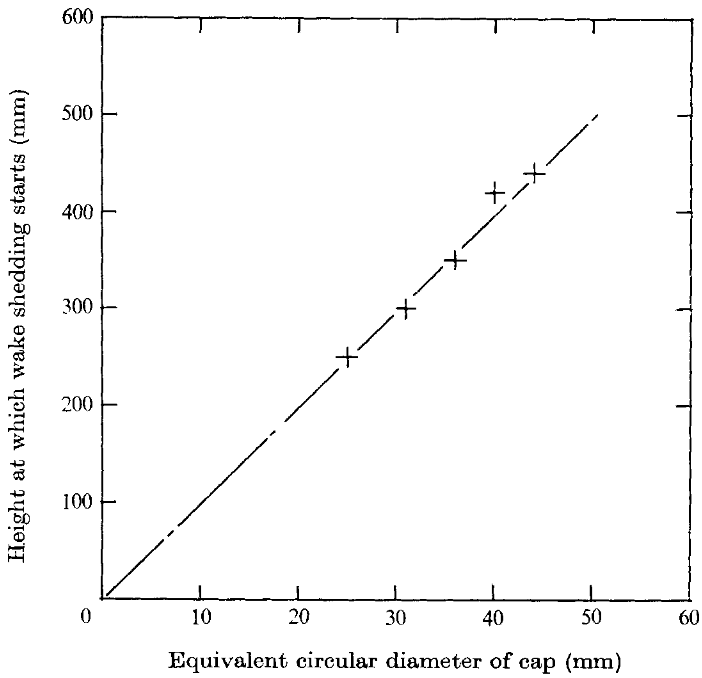

FIGURE 2. Onset of wake shedding.

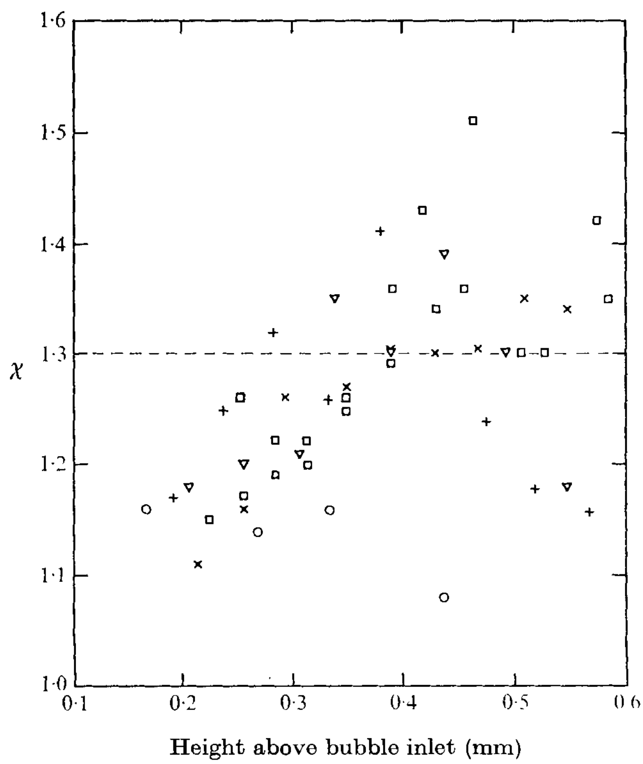

FIGURE 3. Variation of axis ratio with height. ○, 5 ml cap; +, 7·5 ml cap; ▽, 10 ml cap; ×, 12·5 ml cap; □, 15 ml cap.

the horizontal diameter when the wake is being shed, and while there is a slight tendency for χ to increase with bubble size, it is more convenient to use a single value throughout: $\chi = 1{\cdot}3$. This value also fits the photographs of Collins (1965*b*) and of Crabtree & Bridgwater (1967).

3. The elliptical cap

Grace & Harrison (1967) have applied the method of Davies & Taylor to irrotational flow around an ellipse. Their result may be expressed as

$$U = (ag)^{\frac{1}{2}}/(1+\chi). \tag{6}$$

As $\chi \to 1$ the ellipse becomes a circle and (6) reduces to (2).

We have shown that a two-dimensional cap followed by a closed wake forms an oval shape which could well be fitted by an ellipse of appropriate axis ratio. However, in the majority of experimental work, the wake is not visible and it is necessary to determine from the bubble cap alone whether it is an arc of an ellipse or a circle, and then determine the appropriate length parameter (a or R). If arcs of a circle and ellipse of suitable sizes are superimposed (figure 5) it can be seen that, over the 100° arc subtended by a bubble cap, the two curves are scarcely distinguishable, so that either may equally well be fitted to the bubble outline.

The size of the bubble is easily determined by fitting mathematically an appropriate curve through the nose and two points close to the trailing edge. We can fit either a circle of radius R or an ellipse of semi-major axis a and axis ratio χ. Simple trigonometry shows that a and R are related by

$$a/R = \tfrac{1}{2}[1+\chi^2+\cos\theta\,(\chi^2-1)], \tag{7}$$

where 2θ is the angle subtended by the circular arc at its centre. For $\chi = 1{\cdot}3$, a/R is a weak function of θ in the range $0 < \theta < 50°$. Measurements are normally made close to the trailing edge, where $\theta \doteq 50°$, giving $a = 1{\cdot}57R$. Substituting this value for a in (6), with $\chi = 1{\cdot}3$, gives

$$U = 0{\cdot}545(Rg)^{\frac{1}{2}}. \tag{8}$$

Comparison of (8) and (2) shows that the elliptical cap rises 9 % faster than the circular cap of the same apparent size. This exactly explains the discrepancy observed by Collins (1965*a*).

4. Wall effects

An oval shape very similar to an ellipse is formed by the closed streamline of the potential flow due to a source and a sink in a uniform stream. Adapting the analysis of Collins (1965*a*) we can calculate the rise velocity of an elliptical cap bubble between two plane walls, and thus allow for finite bed width.

Lamb (1932, p. 71) gives the complex potential for a source between two parallel planes at $z = \pm\frac{1}{2}iL$. For the combination of a source at $z = +d$ and a sink at $z = -d$, we have

$$w = Uz - m\log\left(\sinh\frac{\pi(z-d)}{L}\right) + m\log\left(\sinh\frac{\pi(z+d)}{L}\right). \tag{9}$$

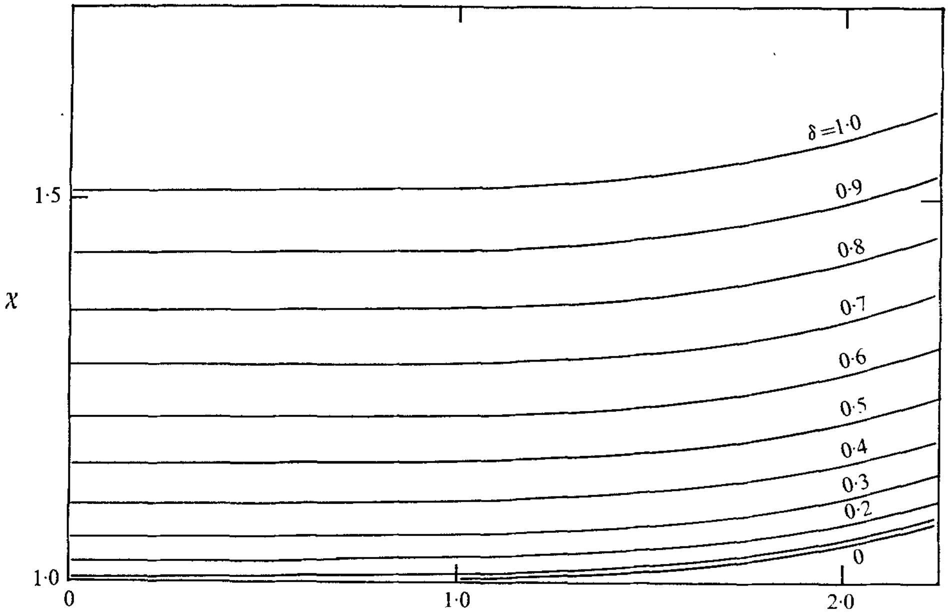

FIGURE 4. Axis ratio as a function of B and δ.

On the dividing streamline Im $(w) = 0$, we find

$$y = \frac{m}{U}\tan^{-1}\left(\frac{\sin Y \sinh D}{\cosh X - \cos Y \cosh D}\right), \tag{10}$$

where $$Y = \frac{2\pi y}{L}, \quad X = \frac{2\pi x}{L}, \quad D = \frac{2\pi d}{L}.$$

Equation (10) represents an oval with major axis along the real axis. If the dimensionless length of the semi-major axis is $A = 2\pi a/L$,

$$\frac{\sin Y \sinh D}{\cosh X - \cos Y \cosh D} = \tan \frac{Y \sinh D}{\cosh A \cosh D}. \tag{11}$$

By substituting for the dimensionless length of the semi-minor axis, $Y = B$ when $X = 0$, we obtain an equation relating A, B and D. All three terms include the column width L, and it is more convenient to separate out the effect of L by writing $$A/B = a/b = \chi, \quad D/B = d/b = \delta.$$

Then $$\frac{\sin B \sinh B\delta}{1 - \cos B \cosh B\delta} = \tan\left(\frac{B \sinh B\delta}{\cosh B\chi - \cosh B\delta}\right). \tag{12}$$

Equation (12) may be regarded as giving, in implicit form, the variation of χ (the axis ratio) with B (inversely proportional to the column width) for various values of the parameter δ. Figure 4 shows the relationship graphically. It can be seen that, for $B < 1{\cdot}2$, χ is virtually independent of B; this means that, except in narrow channels, the channel width does not affect the shape of the oval. The experimental value of $\chi = 1{\cdot}3$ is obtained by setting $\delta = 0{\cdot}730$. Figure 5 presents further confirmation of the insensitivity of the closed-streamline shape to values

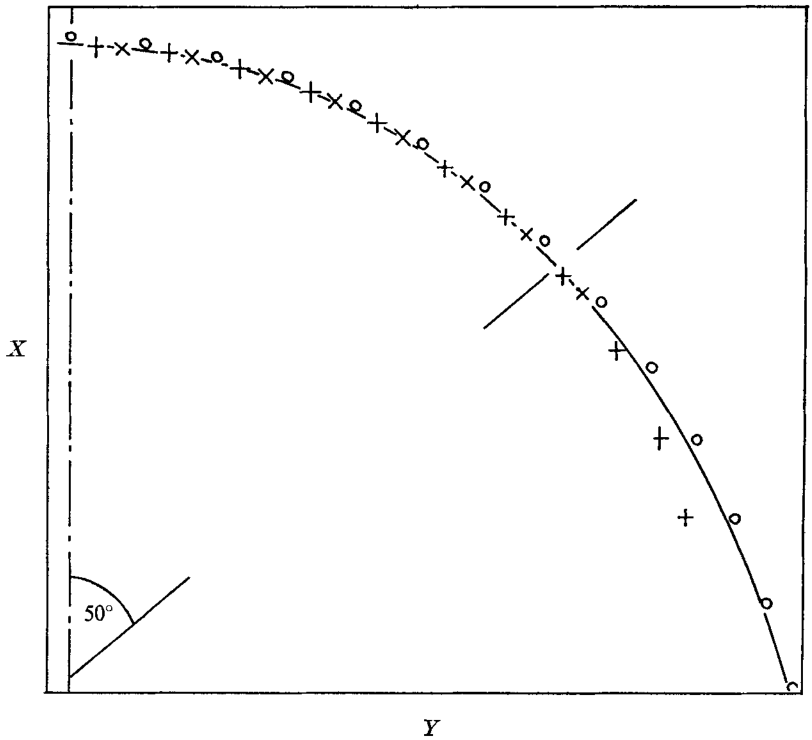

FIGURE 5. Comparison of theoretical shapes. ——, ellipse, $\chi = 1{\cdot}3$; +, circle, $R = 0{\cdot}828$; ○, equation (12), $\chi = 1{\cdot}3$, $\delta = 0{\cdot}730$, $B = 1{\cdot}2$; ×, limit of equation (12), $B \to 0$, $\chi = 1{\cdot}3$, $\delta = 0{\cdot}730$.

of B; it also shows the close similarity between (11) and the ellipse, and between the ellipse and the circle over the 100° arc subtended by the bubbles.

To obtain the theoretical rise velocity, we differentiate (8). After some manipulation, we obtain

$$\frac{dw}{dz} = U\left(\frac{\cosh Z - \cosh A}{\cosh Z - \cosh D}\right). \tag{13}$$

Near to the bubble nose, $X = A - H$ and both H and Y are small. The various terms in (11) may thus be approximated by their series expansions to give

$$\frac{(Y - \frac{1}{6}Y^3)\sinh D}{\cosh(A-H) - (1-\frac{1}{2}Y^2)\cosh D} \simeq \frac{Y\sinh D}{\cosh a - \cosh D} + \frac{1}{3}\left[\frac{Y\sinh D}{\cosh A - \cosh D}\right]^3,$$

whence
$$Y^2 \simeq \frac{6\sinh A\,(\cosh A - \cosh D)}{\cosh^2 A + \cosh A\cosh D - 2}H. \tag{14}$$

The fluid velocity at any point is given by

$$q = |dw/dz| \tag{15}$$

while, from Bernoulli's theorem,

$$q^2 = 2gh. \tag{16}$$

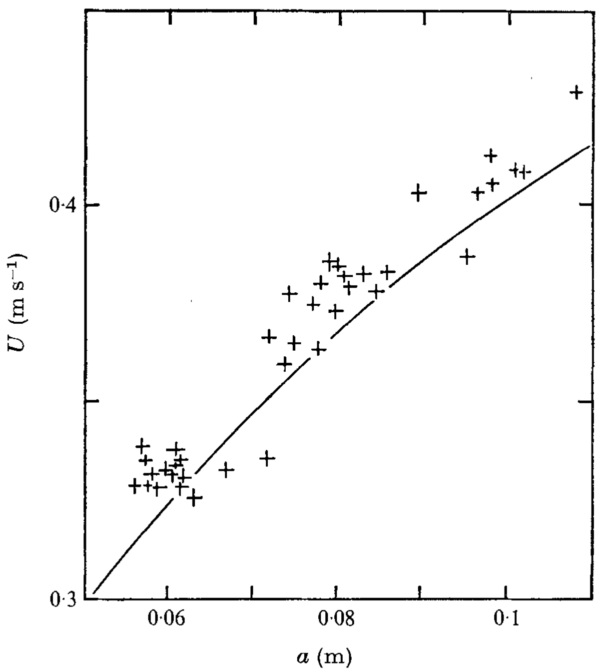

FIGURE 6. Rise velocity of caps in a finite bed.
——, equation (17); +, experiment.

Combining (13)–(16) we obtain

$$U = \left[\frac{(\cosh A - \cosh D)(\cosh^2 A + \cosh A \cosh D - 2)}{\sinh^3 A}\left(\frac{Lg}{6\pi}\right)\right]^{\frac{1}{2}}. \tag{17}$$

It is interesting to study the behaviour of (17) in various limiting cases.

(i) As $d \to 0$. The source and sink become a doublet, the ellipse becomes a circle and (17) reduces to (4).

(ii) As $L \to \infty$ (no wall effect). Equation (17) becomes

$$\left.\begin{aligned} U &= \left[\frac{(\chi^2 - \delta^2)(3\chi^2 - \delta^2)}{12\chi^4}\right]^{\frac{1}{2}}(ag)^{\frac{1}{2}} \\ &= f(\chi)(ag)^{\frac{1}{2}}. \end{aligned}\right\} \tag{18}$$

Numerical calculation of $f(\chi)$ for $\chi = 1{\cdot}3$ and $\delta = 0{\cdot}730$ gives a value of 0·435, which agrees with equation (6) for the ellipse to the third place of decimals. In (18), as $\delta \to 0$ and $\chi \to 1, f(\chi) \to \frac{1}{2}$, which is the value for the unbounded circular cap given in (2).

(iii) As $L \to 0$ (transition to slug flow). Since the source and sink are within the closed curve, $A > D$, whence (17) reduces, in the limit, to (5).

Thus (17) contains all previous results (or very close numerical approximations to them) as special cases.

In the course of some experimental work reported elsewhere (Hills 1971) we measured the rise velocities of bubbles in the column described in §2. Bubbles were photographed at 0·1 s intervals using a rotating slotted disk in front of a fixed camera. Velocities were determined by a least-squares fit of height against time, and bubble sizes by fitting an ellipse of axis ratio 1·3 to three points on the curved upper surface. Average values were used, after rejecting results for the initial transient period. The column width L was constant at 552 mm, and variation in B arose solely through variation in bubble size. The largest value recorded was $B = 0{\cdot}93$, so that all the results lie within the region where χ is independent of B. Figure 6 presents the results as a graph of U *vs*. a. Agreement is seen to be better than that of Collins (1965*a*) or of Grace & Harrison (1967); experimental velocities tend to exceed the theory by about 2 %.

5. Discussion

Modelling the flow above a two-dimensional cap bubble by irrotational flow around an ellipse-like oval leads to a closer agreement with experiment than does using irrotational flow around a circle. The residual discrepancy, of some 2 %, could be due to the three-dimensional character of the actual flow as suggested by Collins (1965*b*). It is not, however, possible to estimate the magnitude of this effect.

A different model flow was proposed by Garabedian (1961) and discussed by Collins (1967). It consists of a cycloidal cap followed by an infinite parallel-sided stagnant wake. The wake is physically unrealistic, but the cap fulfils the boundary condition that the pressure be constant everywhere along the dividing streamline. The elliptical and circular cap models use the much weaker condition that the second derivative of pressure variation should vanish at the forward stagnation point.

Over the 100° arc subtended by a bubble, a cycloidal cap is as good a fit to the experimental shape as a circle or ellipse; if R is the radius of the fitted circle, the rise velocity is given by

$$U = 0{\cdot}51(Rg^{\frac{1}{2}}). \tag{19}$$

Comparison with (2) and (8) shows that this equation fits the experimental results better than that for a circular cap though less well than that for an elliptical one.

It is not known whether the cycloidal cap is the only solution to the two-dimensional free-streamline problem. However, the corresponding three-dimensional problem has no unique solution, and Garabedian (1957) suggested, somewhat arbitrarily, that the correct solution is the one which yields the highest rise velocity.

This maximum velocity principle was used by Grace & Harrison (1967) to explain their measurements on two-dimensional cap bubbles pierced by a vertical rod. Such bubbles are more elongated than unhindered caps and rise faster, and the authors suggested that a bubble adopts that stable shape which has the greatest rise velocity. Elliptical and parabolic caps with major axes vertical rise faster, according to the Davies & Taylor analysis, than circular caps of the same volume, and the greater the elongation, the greater the rise velocity. Somehow the presence of the vertical rod stabilizes the otherwise unstable elongated configuration, permitting the faster rising bubbles to be formed.

We may conjecture that a similar situation holds in our case. Inviscid free-streamline theory permits a variety of flow patterns, of which the cycloidal cap is one. The more elongated shapes have higher rise velocities but are less stable to small perturbations. Stability is provided by viscous effects in the boundary layer over the bubble and its following wake, and the bubble adopts that shape which has the highest rise velocity consistent with stability. In water, this turns out to be more elongated than the cycloidal cap and well described by an ellipse of axis ratio 1·3. The following points may be noted.

(*a*) The axis ratio is unaffected by the thickness of the two-dimensional bed. The same value, $\chi = 1{\cdot}3$, pertains to the photographs of Collins (thickness 6 mm), this work (thickness 10 mm) and Crabtree & Bridgwater (thickness 13 mm). It is thus a true two-dimensional effect, unlike the stability of the vortex pair in the closed wake, which we showed in § 2 to be greater in the narrower bed.

(*b*) Increased liquid viscosity increases the axis ratio. In the photograph of Crabtree & Bridgwater for a water–glycerol mixture of viscosity 10 cP the value is $\chi = 1{\cdot}56$.

(*c*) The effect of bubble size is uncertain. Figure 3 suggests that χ increases with bubble size, but the agreement between theory and experiment shown in figure 6 indicates that the use of a constant value for χ does not give any systematic error.

(*d*) There is no corresponding elongation in the three-dimensional case. The photographs which show a closed wake indicate that it is very closely spherical, and the rise velocity measured experimentally tends, if anything, to be slightly below the theoretical value of Davies & Taylor.

I should like to thank my supervisor, Dr J. F. Davidson, for his help and encouragement during this work, the workshop staff of the Department of Chemical Engineering, Cambridge, for the construction of the apparatus, and Mr D. Pike for the photographs. Financial support was provided in the form of a Research Studentship from the Science Research Council, whose assistance is gratefully acknowledged.

REFERENCES

Collins, R. 1965*a* *J. Fluid Mech.* **22**, 763.

Collins, R. 1965*b* *Chem. Engng Sci.* **20**, 851.

Collins, R. 1967 *Chem. Engng Sci.* **22**, 89.

Collins, R. 1968 Ph.D. thesis, University of London.

Crabtree, J. R. & Bridgwater, J. 1967 *Chem. Engng Sci.* **22**, 1517.

Davies, R. M. & Taylor, G. I. 1950 *Proc. Roy. Soc.* A **200**, 375.

Garabedian, P. R. 1957 *Proc. Roy. Soc.* A **241**, 423.

Garabedian, P. R. 1961 *Modern Mathematics for the Engineer*, p. 365. McGraw-Hill.

Grace, J. R. & Harrison, D. 1967 *Chem. Engng Sci.* **22**, 1337.

Haberman, W. L. & Morton, R. K. 1953 *David Taylor Model Basin Rep.* no. 802.

Hills, J. H. 1971 Ph.D. thesis, University of Cambridge.

Lamb, H. 1932 *Hydrodynamics*, 6th edn. Cambridge University Press.

Maxworthy, T. 1967 *J. Fluid Mech.* **27**, 367.

Moore, D. W. 1959 *J. Fluid Mech.* **6**, 113.

Wegener, P. P. & Parlange, J. Y. 1973 *Ann. Rev. Fluid Mech.* **5**, 79.

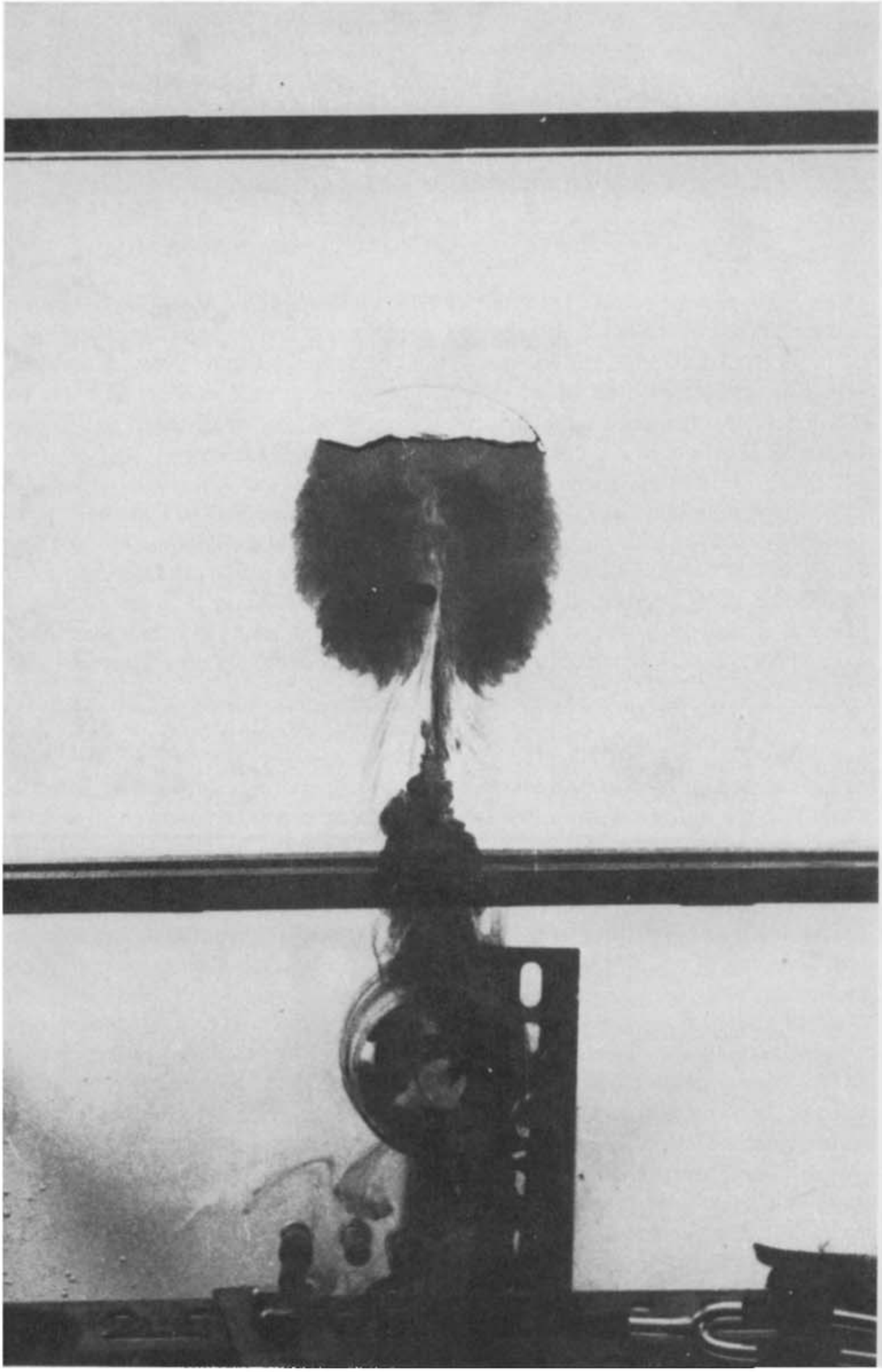

FIGURE 1(*a*). For caption see plate 2.

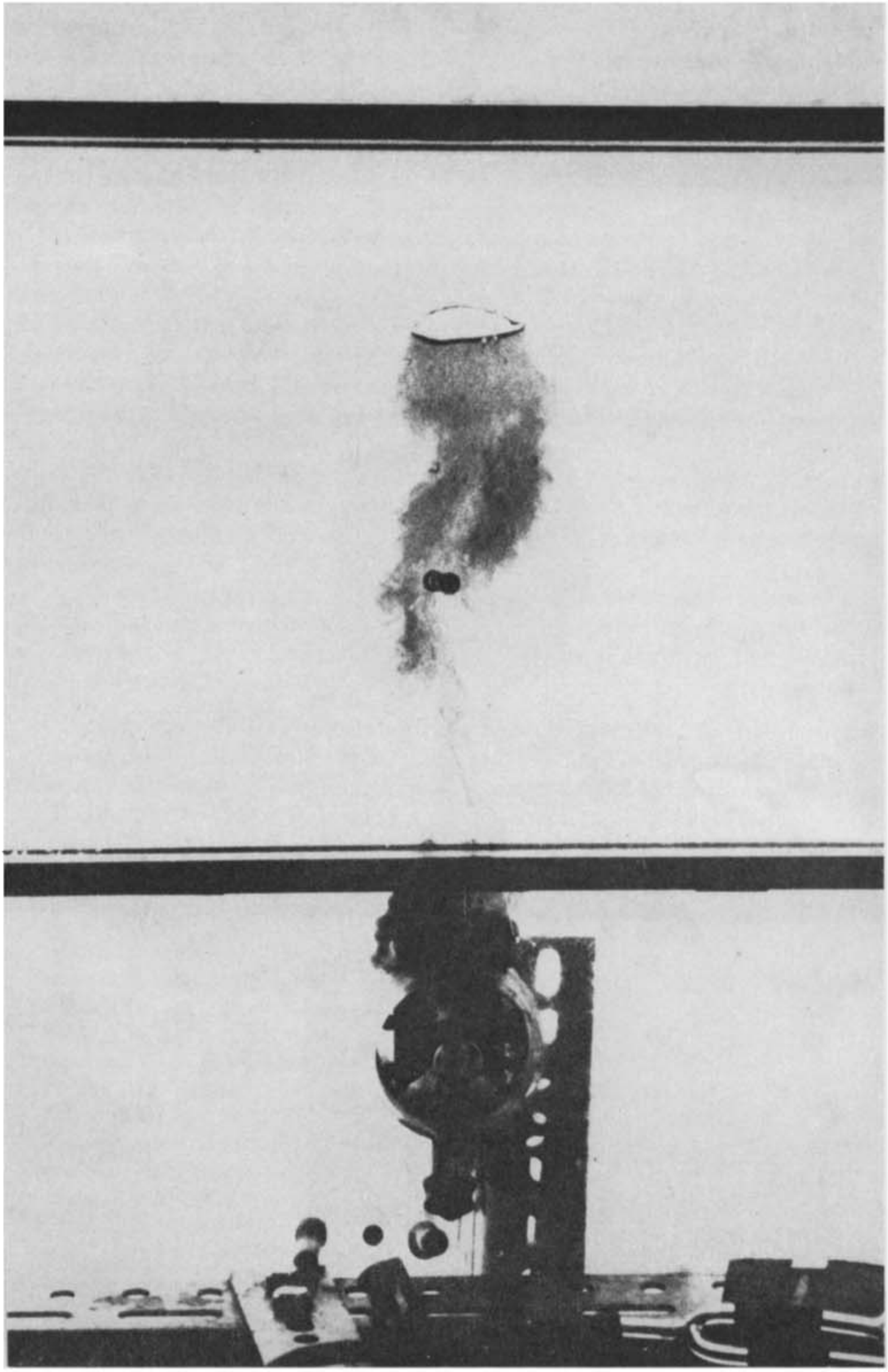

(*b*)

FIGURE 1. Wake of (*a*) a 15 ml cap and (*b*) a 5 ml cap.

HILLS